NACA

RESEARCH MEMORANDUM

THEORETICAL ANALYSIS OF ONE-STAGE WINDMILLS FOR REDUCING FLOW DISTORTION

By Robert E. English and Peggy L. Yohner

Lewis Flight Propulsion Laboratory
Cleveland, Ohio

CLASSIFIED DOCUMENT

NATIONAL ADVISORY COMMITTEE
FOR AERONAUTICS

WASHINGTON
June 12, 1957

NATIONAL ADVISORY COMMITTEE FOR AERONAUTICS

RESEARCH MEMORANDUM

THEORETICAL ANALYSIS OF ONE-STAGE WINDMILLS FOR REDUCING FLOW DISTORTION

By Robert E. English and Peggy L. Yohner

SUMMARY

Isentropic flow and simple radial equilibrium were assumed in analyzing two windmills for reducing flow distortion. The following conclusions and results were obtained: Windmills are inherently limited to flows per unit area lower than those attainable in modern compressor design; at high flows, the uncambered rotor blades must be so thin that blade vibration will be a critical problem. Windmills reduced velocity distortions 20 to 38 percent and total-pressure distortions 22 to 43 percent. The design value of the ratio of axial velocity to blade tip speed appears to have a greater effect on the amount of distortion reduction than the other variables investigated. For inlet velocity distortions as great as 0.80, the angles of incidence were near 20°, although the diffusion factors were only about 0.2. In reducing velocity distortion, windmills transfer energy from one portion of the stream to another and thereby introduce a distortion of total temperature; total-temperature distortions of 2 to 5 percent were introduced by these windmills.

INTRODUCTION

Distortion of engine-inlet airflow is, broadly speaking, any departure from steady-state conditions of purely axial flow (no whirl) and of constant total pressure and total temperature over the exit from the inlet diffuser. Distortion of flow at the exit of supersonic inlet diffusers impairs performance of turbojet engines following these inlets. The magnitude of these performance penalties is indicated by references 1 to 7. Reduction of these distortions by improved inlet design and by relocation of distortion-producing devices such as guns and rockets is currently receiving considerable attention; use of distortion-reducing devices such as screens is also being considered (refs. 8 and 9). Another device for reducing flow distortion is a windmilling rotor followed by a set of straightening vanes, hereinafter called a "windmill." Windmills are currently being evaluated both experimentally and theoretically at the NACA Lewis laboratory as part of a broad program of distortion reduction.

Early work on windmills is reported in references 10 and 11. In each of these reported studies, rotating blade rows were used without either preceding or following stator blade rows. In reference 11, windmills having either a single rotor blade row or two counterrotating blade rows were investigated. Each of these references, in which flow velocities of 100 feet per second or less were investigated, shows that velocity in ducts may be made more uniform by use of a windmill. References 8 and 9 present some results from tests of a one-stage windmill for which the inlet axial Mach number was as great as 0.55.

The study described herein is confined to an analysis of windmills consisting of one row of freely moving rotor blades followed by a single row of stationary blades. Windmill geometry is schematically illustrated in figure 1. The function of the stator blades is to straighten the exit flow and thereby to remove whirl that either is introduced by the rotor or is present upstream of the windmill. The general purposes of this analysis are to investigate (1) the inherent characteristics and limitations of windmills, (2) the variation in flow directions and velocities within such a device, and (3) the maximum reduction in radial flow distortion that can conceivably be effected by a one-stage windmill with high subsonic inlet flow Mach numbers. This analysis is confined to a study of radial variation in total pressure. Total temperature is considered to be constant ahead of the windmill, and the flow is assumed to be both axial and steady with respect to time.

GENERAL PRINCIPLES

In a straight duct, steady axial flow of gas having constant total temperature is characterized by constant static pressure. In addition, when there is a variation in total pressure, it is reflected in a variation in axial velocity. The purpose of a windmill is to extract energy from the high-velocity part of the stream and to add this energy to the low-velocity part of the stream. In this way, the axial velocity is made more uniform by the windmill.

It is desired that the windmill not distort uniform flow. This desire has resulted in basically the same simple rotor design in references 8 to 11 and in this analysis: The rotor blades are considered to be symmetrical uncambered airfoils having a stagger angle β_d of

$$\beta_d = -\tan^{-1}\left(\frac{U}{V_z}\right)_d \tag{B3}$$

It is also desirable that the windmill, in eliminating or reducing one distortion, should not introduce another distortion. In particular, as a windmilling rotor removes energy from the high-velocity portion of the stream and adds it to the low-velocity portion, the resulting

tangential forces on the gas introduce tangential velocities; such a distortion of tangential velocity should be removed before the gas leaves the windmill. In a one-rotor windmill, a row of stator blades downstream of the rotor will fulfill this function. In order that these stator blades not distort uniform flow, they are herein selected to be uncambered symmetrical airfoils with zero stagger.

The extraction of energy from the high-velocity part of the stream by the windmill reduces the total temperature of this part of the stream and correspondingly increases the total temperature of the low-velocity part of the stream. This distortion of total temperature is an inherent characteristic of windmills; they are therefore incapable, even ideally, of completely eliminating distortion from distorted flows.

The angle of incidence on the windmill rotor blades and thus the aerodynamic forces on the blades vary with distortion of axial velocity. For example, hypothesize a one-stage windmill (one rotor blade row followed by one stator blade row) that reduces but does not eliminate distortion of axial velocity. A reasonable extension of this hypothesis is that successive windmill stages will further reduce distortion of axial velocity. As the magnitude of this distortion is progressively reduced, the angles of incidence on the successive windmill stages diminish. The decrease in aerodynamic loading that accompanies reduction in angle of incidence results in less and less correction of the distorted flow as the distortion decreases. Apparently, then, use of increasing numbers of independent windmill stages will ideally cause the axial velocity to approach a constant value asymptotically. In the absence of mixing, the ultimate result attainable by a series of windmills is constant axial velocity, zero tangential velocity, and a distortion of total temperature.

Since windmills appear incapable of completely eliminating flow distortion, some other basis is required for evaluating windmills. The variation in total temperature introduced by the windmill is accompanied by a variation in total pressure. Thus it is evident that constant total pressure, in particular, should not be the basis on which windmills are evaluated. On the other hand, the ideal condition that a series of windmills approaches (i.e., constant axial velocity) appears to be an appropriate basis of evaluation.

This hypothetical condition of constant axial velocity and distorted total temperature provides the angles of incidence on the first compressor rotor blade row (without inlet guide vanes) corresponding to zero distortion. However, the distortion of total temperature at the compressor inlet will result in a velocity distortion at the exit of the first compressor stage; this velocity distortion is accompanied by distortion of angle of incidence on the second rotor blade row. It appears that, even if velocity distortion at the compressor inlet can be largely eliminated by a windmill, the resulting distortion of total temperature may impair compressor performance in succeeding stages.

SCOPE OF ANALYSIS

General Conditions

Axially symmetric flow through one rotor blade row and one stator blade row was considered in the analysis. In other words, flow ahead of the windmill was assumed to have only radial distortion. For each selected flow distortion, a set of operating conditions was determined by successive trials that resulted in zero power input or output from the windmill. For any given set of inlet gas conditions and steady-state operation, a windmill has only one degree of freedom (e.g., rotational speed). In the analysis, mass flow was varied for an assigned value of rotational speed until the net power output of the windmill was zero.

At any given radial position, the direction of relative flow leaving a blade row was assumed to be the same as the relative flow direction with no distortion. The entropy of any given particle was assumed to be unchanged by its passage through the windmill. The blades were assumed to be tightly packed (high solidity) so that the air can reasonably be assumed to flow along circular surfaces without the twisting and mixing of secondary flows.

Symbols are defined in appendix A, and the method of analysis is outlined in appendix B.

Windmill Design

The windmill designs can be described in terms of two velocity-diagram variables employed in this analysis: (1) hub-tip radius ratio r_h/r_t, and (2) ratio of axial velocity to blade tip speed, hereinafter called axial velocity ratio $(V_z/U_t)_d$. Hub-tip radius ratio was assigned the value of 0.4 and was kept constant from entrance to exit of the windmill. Axial velocity ratio $(V_z/U_t)_d$ was chosen to be either 0.7 or 1.0.

Flow Conditions

Six specific combinations of conditions were investigated (table I). For each of the two axial velocity ratios, two equivalent blade speeds were assigned, one corresponding to a zero-distortion axial Mach number of 0.5 and the other to 0.7. Distortions having low velocity at either rotor tip or rotor hub were considered. The six cases considered are summarized in the following table:

Case	1	2	3	4	5	6
Design axial velocity ratio, $(V_z/U_t)_d$	0.7	0.7	0.7	1.0	1.0	1.0
Equivalent blade speed, $U_t/\sqrt{\theta_1}$, ft/sec	1066	1066	778	746	746	545
Radius with low velocity	Hub	Tip	Hub	Hub	Tip	Hub
Rotor-inlet total-pressure distortion, $(\Delta P/P_{av})_1$	0.476	0.505	0.237	0.474	0.502	0.237

The radial distributions of velocity were arbitrarily selected. The particular method of analysis (appendix B) requires assignment of radial distribution of entropy at the rotor exit rather than at the windmill entrance. These radial distributions of entropy were chosen to give a velocity that varies linearly with radius, except for radial shifts in mass flow through the rotor.

RESULTS

The results for the six cases investigated are summarized in table II. Because the axial velocity ratios $(V_z/U_t)_d$ are the same for cases 1 to 3, the geometry of these windmills is the same. Similarly, cases 4 to 6 all have the same geometry. The results can thus be interpreted as those of two windmills, each operated under three sets of operating conditions.

The amounts of distortion reduction in axial velocity and total pressure are of great interest. For cases 1 to 3, the velocity distortion is reduced 34 to 38 percent, and the total-pressure distortion 34 to 43 percent. For cases 4 to 6, 20 to 24 percent of the velocity distortion and 22 to 29 percent of the total-pressure distortion are eliminated. The amount of distortion elimination appears to vary more with the axial velocity ratio $(V_z/U_t)_d$ than with the blade speed $U_t/\sqrt{\theta_1}$ or with the radius having the low velocity. The rotor blade mean stagger angle is 45° for cases 1 to 3 and 35° for cases 4 to 6. Smaller reduction in distortion with a mean stagger of 35° (cases 4 to 6) is in agreement with the observations in reference 11.

For each design, low velocity at the hub radius receives greater velocity-distortion correction than low velocity at the tip radius receives, but this greater correction is accompanied by more severe flow conditions. With low velocity at the hub radius, the diffusion factors, incidence angles, and rotor-inlet Mach numbers are all increased.

Although none of the diffusion factors exceeds 0.2, the angles of incidence can be almost 20°. The magnitudes of D are well within

current limits on compressor design, but the incidence angles are outside currently acceptable limits. The high incidence angles are especially undesirable because they are accompanied by high rotor-inlet relative Mach numbers. If the low-velocity region is at the tip radius, the incidence angles are at a more reasonable level. The radial variation of angle of incidence is shown in figure 2. As was anticipated from the assigned inlet distortion, the angles of incidence change sign from one end of the blades to the other.

The rotor-inlet relative Mach numbers also appear to be a potential source of trouble for those cases having a design axial Mach number of 0.7 (see fig. 3(a), cases 1, 2, 4, and 5). For case 2, in particular, rotor-inlet relative Mach number is near 1.0 over the whole blade height, resulting in especially severe flow conditions for small incidence angles on the uncambered rotor blades. This problem will be further amplified in the DISCUSSION.

The exit equivalent airflow shown in table II varies from 29 to 39 pounds per second - square foot.

A small rise in static pressure across the windmill results from the general leveling out of the velocity across the windmill. The values of total-pressure ratio $P_{av,3}/P_{av,1}$ are greater than 1.0 in spite of the assumption of constant entropy along each streamline. This variation in total pressure is a consequence of the definition of average total pressure used in this analysis (see refs. 12 and 13 for discussion of this problem). Average total pressure is herein defined as that total pressure required with uniform flow to pass the observed mass flow per unit area with the observed static pressure and mass-averaged total temperature of the stream. The variation in average total pressure across the windmill reflects the fact that such an average total pressure is not a unique function of the energy content and entropy of the stream, for each of these quantities remains constant.

Exit total temperature varies from 2 to 5 percent along the radius. Total temperature is shown in figure 4 to vary considerably over the annulus except near the hub radius, where the energy addition or extraction levels off and in some cases even decreases. This is apparently a result of the fact that the falling blade speed near the hub reduces the potential work capacity of the rotor blades; this effect can be illustrated by considering the extreme case of zero hub radius, for which the blade hub speed and hence the work capacity at the hub for any finite gas velocity would be zero.

Profiles of axial velocity and total pressure typical of those obtained in this analysis are presented in figures 5 to 8. Effects of varying both the mass flow and the radius having the low velocity are shown. Variation in axial velocity with radius at the windmill entrance

is not quite linear, because entropy is specified at the rotor exit rather than at the entrance. The shape of the curves is different for plots against radius and against mass flow. This difference results in part from the variation in annular area with radius and in part from the variation in flow per unit area with axial velocity. Because of radial displacement of flow in passing through the windmill, intersections of corresponding curves do not represent related points in the flow field.

4072

For case 1, the varying axial velocity and total pressure at the windmill inlet are significantly flattened at the windmill exit, especially at the tip radius. Reducing the mass flow to that of case 3 changes the magnitudes but not the general character of the curves (figs. 5(a), 6(a), 7(a), and 8(a)). Moving the region of low velocity from the hub to the tip (figs. 5(b), 6(b), 7(b), and 8(b)) reduces the disparity between hub and tip in their ability to reduce distortion. Table II shows that moving the low velocity to the tip radius reduces diffusion factors and angles of incidence.

DISCUSSION

Although a one-stage windmill appears to be capable ideally of reducing velocity and total-pressure distortions 30 to 40 percent, several problems arise in the use of windmills of high flow capacity. The principal source of this difficulty is choking within the rotor blade passages. Consider the design conditions of the windmills analyzed in cases 1 to 6; their design operating conditions without any inlet distortion are summarized in table I. The rotor-inlet relative Mach numbers are such that, for cases 1, 2, 4, and 5, the critical-area ratios A_{cr}/A are 1.0 or only slightly less. In order that the over-all effect of these high values of critical-area ratio could be better assessed, the margin of area over that required for choking was integrated over the annular area. The result is the average critical-area ratio $(A_{cr}/A)_{av}$ in table I.

Cases 1 and 2 can permit only a 1.2-percent reduction in annular area before the passing of the design mass flow becomes a physical impossibility. This imposes a severe restriction on rotor blade thickness that is more extreme than that for a comparable axial-flow compressor because the rotor blades of the windmill are uncambered and are designed for zero incidence angles. The camber and the incidence angles of compressor rotor blades both permit thicker blades by tending to produce a widening of the cross-channel width between blades over that occupied by the flow ahead of the rotor blade row. Low blade thickness would subject the windmills to vibrational difficulties. The camber as well as the thickness of typical compressor blades increases the section modulus and thereby stiffens the blades, whereas blades in a windmill must obtain all their stiffness from profile thickness.

The average critical-area ratio of cases 1 and 2 could be reduced by lowering the rotor-inlet relative Mach number. (Raising the rotor-inlet Mach number above 1.0 can also reduce critical-area ratio, but this is generally a less practical solution.) Some adjustments that might be made by lowering that Mach number are illustrated in table I. Decreasing blade speed 30 percent to that of cases 4 and 5 helps hardly at all; as table II shows, this reduction in blade speed is probably accompanied by significant reduction in ability to eliminate distortion.

Lowering the axial Mach number to 0.5 as in cases 3 and 6 offers greater reduction in average critical-area ratio (table I). In particular, if axial Mach number is decreased without reducing the design axial velocity ratio $(V_z/U_t)_d$, the ability to reduce distortion is not impaired; in fact, more velocity distortion is eliminated. The penalty associated with the lowered axial Mach number is a concomitant reduction in flow capacity. Thus windmills appear to be limited by blade structural requirements to flows per unit area lower than those obtainable in modern compressor design.

Reduction in blade-row-inlet Mach number will not only permit increasing rotor blade thickness but will also increase the range over which incidence angle can vary efficiently. The particular angles of incidence obtained in this analysis are associated with the particular distortions assumed. A windmill should have smaller incidence angles with distortion than corresponding compressors because of the automatic adjustment in blade speed that accompanies a change in axial velocity or equivalent weight flow through the windmill. Adjustment of rotor blade speed to a condition of zero (or near zero) net torque keeps the lift coefficients and incidence angles low. This is in contrast to the high incidence angles and high blade loadings typically acquired by inlet stages of multistage compressors during operation at low equivalent rotational speed. Thus windmills are aerodynamically capable of accepting a wider range of inlet-flow distortion than are compressors.

The primary function of a windmill is to transfer energy from one part of a stream to another by extracting work and injecting work in equal quantities. Although secondary flows will inevitably introduce some mixing, this mixing appears to be a less important characteristic of a windmill.

CONCLUSIONS

Two windmill designs for reducing flow distortion were analyzed; isentropic flow and simple radial equilibrium were assumed. It was concluded that windmills are inherently limited to flows per unit area lower than those attainable in modern compressor design; at high flows, the uncambered rotor blades must be so thin that blade vibration will be critical.

Because transfer of energy from one portion of the stream to another distorts total temperature, windmills are incapable, even ideally, of completely eliminating distortion.

Analysis of each of the windmills for three sets of operating conditions gave the following results:

1. Velocity distortions were reduced 20 to 38 percent.

2. Total-pressure distortions were reduced 22 to 43 percent.

3. Total-temperature distortions of 2 to 5 percent were introduced by the windmill.

4. The design value of the ratio of axial velocity to blade tip speed appears to have a greater effect on amount of distortion reduction than the other variables investigated.

5. For inlet velocity distortions as great as 0.80, the angles of incidence were near 20°, although the diffusion factors were only about 0.2.

Lewis Flight Propulsion Laboratory
National Advisory Committee for Aeronautics
Cleveland, Ohio, April 10, 1957

APPENDIX A

SYMBOLS

A	area, sq ft
$a_{a,cr}$	critical velocity $\sqrt{\frac{2\gamma}{\gamma+1} gRT}$, ft/sec
c_p	specific heat at constant pressure, Btu/(lb)($^\circ$R)
D	diffusion factor (see eq. (B12))
g	standard gravitational acceleration, 32.17 ft/sec^2
i	incidence angle, angle between inlet-air direction and tangent to blade mean camber line at leading edge, deg
J	mechanical equivalent of heat, 778.16 ft-lb/Btu
M	Mach number
P	absolute total pressure, lb/sq ft
$\mathscr{P}$	power, ft-lb/sec
p	absolute static pressure, lb/sq ft
R	gas constant, 53.38 ft-lb/(lb)($^\circ$R)
r	radius, ft
S	entropy, Btu/(lb)($^\circ$R)
T	total temperature, $^\circ$R
U	blade speed, ft/sec
V	gas velocity, ft/sec
w	mass-flow rate of gas, lb/sec
β	flow direction relative to rotor, deg
β_d	rotor stagger angle, deg
γ	ratio of specific heats

δ ratio of pressure to NACA standard sea-level pressure of 2116 lb/sq ft

θ ratio of temperature to NACA standard sea-level temperature of 518.7° R

ρ gas density, lb/cu ft

σ solidity, ratio of chord to spacing

ω angular velocity, radians/sec

Subscripts:

a stagnation condition

av average

cr critical or choking

d design

h hub

m mean

R rotor

S stator

t tip

z axial component

θ tangential component

1 rotor inlet

2 rotor exit and stator inlet

3 stator exit

Superscript:

' relative to rotor

APPENDIX B

METHOD OF ANALYSIS

The following conditions were assumed to prevail:

(1) Along each streamline, the flow is isentropic.

(2) In the axial spaces upstream and downstream of blade rows, the flow is in simple radial equilibrium; that is,

$$\frac{dp}{dr} = \frac{\rho V_\theta^2}{gr} \tag{B1}$$

(3) The blades are so closely spaced that the fluid flows along surfaces of revolution about the axis of rotation and at any given radius the direction of flow relative to either blade row is constant at the blade-row exit and parallel with a tangent to the mean camber line at the trailing edge.

(4) No net power is supplied to or taken from the rotor, that is,

$$\mathscr{P} = \frac{\omega}{g}\int_{hub}^{tip} (r_1 V_{\theta,1} - r_2 V_{\theta,2})\, dw = 0 \tag{B2}$$

(5) The tangential velocity of the entering stream is zero, and its total temperature is constant.

(6) All conditions are steady with respect to time.

(7) The blades are symmetrical uncambered airfoils. The stator blades have zero stagger, and the stagger angle of the rotor blades is given by

$$\beta_d = -\tan^{-1}\left(\frac{U}{V_z}\right)_d \tag{B3}$$

The physical arrangement of the parts and the axial stations are shown in figure 1.

From the definition of total state,

$$c_p(T_1 - T_1') = \frac{2U_1 V_{\theta,1} - U_1^2}{2gJ} \tag{B4}$$

If a given streamline shifts in radius in passing through the rotor, its total temperature relative to the rotor T' changes in the following way:

$$c_p(T_2' - T_1') = \frac{U_2^2 - U_1^2}{2gJ} \tag{B5}$$

Subtraction of equation (B4) from (B5) yields

$$c_p(T_2' - T_1) = \frac{U_2^2 - 2U_1V_{\theta,1}}{2gJ}$$

Since the initial tangential velocity $V_{\theta,1}$ was assumed to be zero, this expression reduces to

$$c_p(T_2' - T_1) = \frac{U_2^2}{2gJ} \tag{B6}$$

For any assigned inlet total temperature T_1, which was assumed to be constant along the radius, and an assigned rotational speed ω, the relative total temperature T_2' is a simple function of radius and is independent of both inlet axial-velocity distortion and the amount of radial displacement in passing through the rotor. This fact was helpful in the analysis, because there was no need to estimate the radial displacements and correct the estimates by successive trials. Instead, entropy distribution was assigned at the rotor exit (station 2), and the radial shift in the blade rows and the inlet and exit distortions were made dependent upon the assigned entropy distribution at the rotor exit.

Relative total pressure P_2' at the rotor exit can be stated as

$$P_2' = P_{2,m}'\left(\frac{T'}{T_m'}\right)_2^{\frac{\gamma}{\gamma-1}} \exp\left[\frac{J(S_m - S)_2}{R}\right] \tag{B7}$$

where T_2' (from eq. (B6)) and S_2 (by assignment) are both known functions of r_2.

Critical velocity is defined

$$a_{a,cr} = \sqrt{\frac{2\gamma}{\gamma+1} gRT} \tag{B8}$$

For zero inlet tangential velocity, Euler's work equation becomes

$$\frac{U_2 V_{\theta,2}}{gJ} = c_p(T_2 - T_1) \tag{B9}$$

With the aid of trigonometry of the velocity diagrams and some algebraic manipulation, combination of equations (B1) and (B6) to (B9) yields

$$-\frac{d\left(\frac{V_2'}{a_{a,cr,1}}\right)}{d\left(\frac{r_2}{r_t}\right)} = \frac{r_t}{r_2}\frac{V_2'}{a_{a,cr,1}}\sin^2\beta_{d,2} + 2(\sin\beta_{d,2})\frac{U_t}{a_{a,cr,1}} + \frac{a_{a,cr,1}}{V_2'}\left[1 + \frac{\gamma-1}{\gamma+1}\left(\frac{U_t}{a_{a,cr,1}}\right)^2\left(\frac{r_2}{r_t}\right)^2 - \frac{\gamma-1}{\gamma+1}\left(\frac{V_2'}{a_{a,cr,1}}\right)^2\right]\frac{\gamma+1}{2\gamma}\frac{J}{R}\frac{dS_2}{d\left(\frac{r_2}{r_t}\right)} \tag{B10}$$

The important feature of this equation is that it expresses

$$\frac{d\left(\frac{V_2'}{a_{a,cr,1}}\right)}{d\left(\frac{r_2}{r_t}\right)} = f\left[\gamma, \frac{r_2}{r_t}, \beta_{d,2}, \frac{V_2'}{a_{a,cr,1}}, \frac{U_t}{a_{a,cr,1}}, \frac{dS_2}{d\left(\frac{r_2}{r_t}\right)}\right]$$

all of which variables were treated as independent and thus assignable in the calculations, except $V_2'/a_{a,cr,1}$.

Equation (B10) was solved in the following way: The value of $(V_2'/a_{a,cr,1})_m$ was estimated. The resulting rotor-exit flow conditions were then substituted into the following modification of equation (B2) for zero initial tangential velocity:

$$\frac{g\mathscr{P}}{2\pi r_t^2 \rho_{a,1,h} a_{a,cr,1}^3} = -\int_{\frac{r_h}{r_t}}^{1} \frac{U_t}{a_{a,cr,1}}\frac{V_{\theta,2}}{a_{a,cr,1}}\frac{\rho_2 V_{z,2}}{\rho_{a,1,h} a_{a,cr,1}}\left(\frac{r_2}{r_t}\right)^2 d\left(\frac{r_2}{r_t}\right) \tag{B11}$$

The estimated value of $(V_2'/a_{a,cr,1})_m$ was successively altered until the integral in equation (B11) was zero.

For the windmill inlet and outlet (stations 1 and 3), the static pressures $p_{1,h}$ and $p_{3,h}$ were estimated and successively adjusted until the mass flowing past station 2 would just fill the annulus at stations 1 and 3. The last results completed the solution.

The rotor and stator diffusion factors D are defined as follows:

$$\left.\begin{aligned} D_R &\equiv 1 - \frac{V_2'}{V_1'} + \frac{|V_{\theta,2}|}{2\sigma_R V_1'} \\ D_S &\equiv 1 - \frac{V_3}{V_2} + \frac{|V_{\theta,2}|}{2\sigma_S V_2} \end{aligned}\right\} \quad \text{(B12)}$$

The hub solidities $\sigma_{R,h}$ and $\sigma_{S,h}$ were assigned the value of 2.0.

REFERENCES

1. Conrad, E. William, and Sobolewski, Adam E.: Investigation of Effects of Inlet-Air Velocity Distortion on Performance of Turbojet Engine. NACA RM E50G11, 1950.

2. Wallner, Lewis E., Conrad, E. William, and Prince, William R.: Effect of Uneven Air-Flow Distribution to the Twin Inlets of an Axial-Flow Turbojet Engine. NACA RM E52K06, 1953.

3. Walker, Curtis L., Sivo, Joseph N., and Jansen, Emmert T.: Effect of Unequal Air-Flow Distribution from Twin Inlet Ducts on Performance of an Axial-Flow Turbojet Engine. NACA RM E54E13, 1954.

4. Harry, David P., III, and Lubick, Robert J.: Inlet-Air Distortion Effects on Stall, Surge, and Acceleration Margin of a Turbojet Engine Equipped with Variable Compressor Inlet Guide Vanes. NACA RM E54K26, 1955.

5. Huntley, S. C., Sivo, Joseph N., and Walker, Curtis L.: Effect of Circumferential Total-Pressure Gradients Typical of Single-Inlet Duct Installations on Performance of an Axial-Flow Turbojet Engine. NACA RM E54K26a, 1955.

6. Conrad, E. William, Hanson, Morgan P., and McAulay, John E.: Effect of Inlet-Air-Flow Distortion on Steady-State Altitude Performance of an Axial-Flow Turbojet Engine. NACA RM E55A04, 1955.

7. Fenn, David B., and Sivo, Joseph N.: Effect of Inlet Flow Distortion on Compressor Stall and Acceleration Characteristics of a J65-B-3 Turbojet Engine. NACA RM E55F20, 1955.

8. Piercy, Thomas G.: Factors Affecting Flow Distortions Produced by Supersonic Inlets. NACA RM E55L19, 1956.

9. Sterbentz, William H.: Factors Controlling Air-Inlet Flow Distortions. NACA RM E56A30, 1956.

10. Collar, A. R.: The Use of a Freely Rotating Windmill to Improve the Flow in a Wind Tunnel. R. & M. No. 1866, British ARC, Nov. 23, 1938.

11. Johnston, I. H.: The Use of Freely Rotating Blade Rows to Improve Velocity Distribution in an Annulus. Memo. No. M.109, British NGTE, Feb. 1951.

12. Wyatt, DeMarquis D.: Analysis of Errors Introduced by Several Methods of Weighting Nonuniform Duct Flows. NACA TN 3400, 1955.

13. McLafferty, G. H.: A Generalized Approach to the Definition of Average Flow Quantities in Nonuniform Streams. Rep. No. R-13534-9, Res. Dept., United Aircraft Corp., July 20, 1954.

TABLE I. - DESIGN CHARACTERISTICS

[Hub-tip radius ratio, r_h/r_t, 0.4.]

Case	1	2	3	4	5	6
Design axial velocity ratio, $(V_z/U_t)_d$	0.7	0.7	0.7	1.0	1.0	1.0
Equivalent blade speed, $U_t/\sqrt{\theta_1}$, ft/sec	1066	1066	778	746	746	545
Design axial Mach number, $M_{z,d}$	0.7	0.7	0.5	0.7	0.7	0.5
Radius with low velocity	Hub	Tip	Hub	Hub	Tip	Hub
Rotor-inlet mass flow, $w\sqrt{\theta_1}/\delta_1 A_t$, (lb/sec)/sq ft	37.9	37.9	31.0	37.9	37.9	31.0
Rotor-inlet relative Mach number, M_1' Hub	0.81	0.81	0.58	0.75	0.75	0.54
Mean	.99	.99	.71	.85	.85	.61
Tip	1.22	1.22	.87	.99	.99	.71
Critical-area ratio, A_{cr}/A Hub	0.966	0.966	0.821	0.943	0.943	0.786
Mean	1.000	1.000	.918	.981	.981	.850
Tip	.964	.964	.985	1.000	1.000	.918
Average critical-area ratio $(A_{cr}/A)_{av}$	0.988	0.988	0.923	0.981	0.981	0.858

TABLE II. - SUMMARY OF RESULTS

Case	1	2	3	4	5	6
Rotor-inlet velocity distortion, $(\Delta V/V_{av})_1$	0.729	0.548	0.762	0.804	0.552	0.821
Stator-exit velocity distortion, $(\Delta V/V_{av})_3$	.484	.360	.472	.647	.427	.626
Velocity distortion eliminated, %	33.6	34.3	38.1	19.5	22.6	23.8
Rotor-inlet total-pressure distortion, $(\Delta P/P_{av})_1$	0.476	0.505	0.237	0.474	0.502	0.237
Stator-exit total-pressure distortion, $(\Delta P/P_{av})_3$	.271	.334	.136	.336	.393	.168
Total-pressure distortion eliminated, %	43.1	33.9	42.6	29.1	21.7	29.1
Stator-exit total-temperature distortion, $\Delta T_3/T_1$	0.053	0.045	0.028	0.036	0.030	0.019
Max. rotor diffusion factor, D_R	0.17	0.06	0.14	0.19	0.08	0.15
Max. stator diffusion factor, D_S	.13	.08	.12	.14	.08	.13
Max. angle of incidence on rotor, i_R, deg	15.0	-7.7	16.4	16.7	-5.9	17.2
Max. angle of incidence on stator, i_S, deg	18.4	-7.4	17.8	19.6	7.3	18.6
Max. rotor-inlet relative Mach number, M_1'	1.40	1.14	0.98	1.17	1.07	0.82
Max. stator-inlet Mach number, M_2	.78	.96	.55	.81	.99	.57
Stator-exit mass flow, $w\sqrt{\theta_1}/\delta_{av,3}A_t$, (lb/sec)/sq ft	36.6	38.4	29.6	36.2	38.6	29.1
Total-pressure ratio, $P_{av,3}/P_{av,1}$	1.026	1.017	1.015	1.018	1.011	1.012
Static-pressure ratio, p_3/p_1	1.058	1.044	1.021	1.040	1.030	1.016

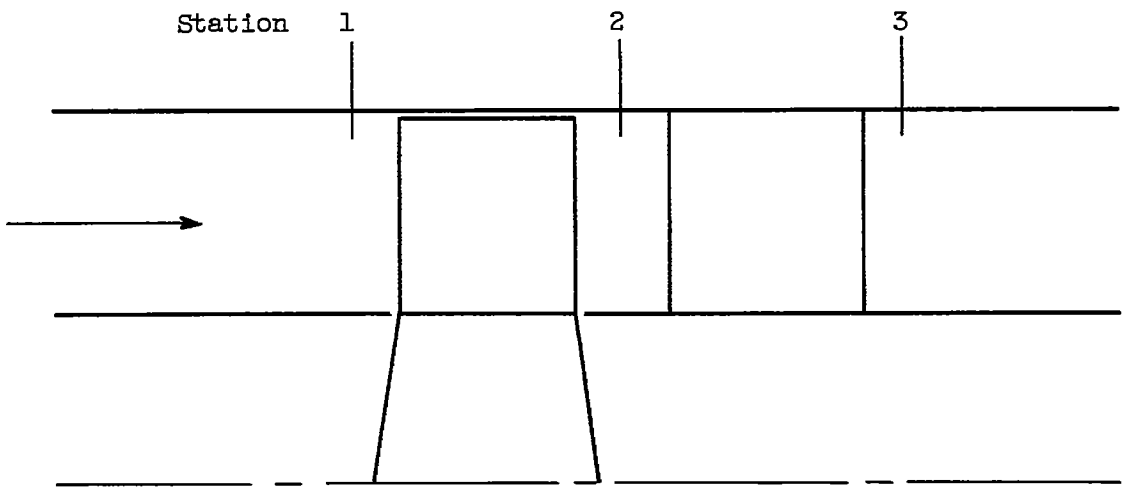

Figure 1. - Schematic arrangement of one-stage windmill.

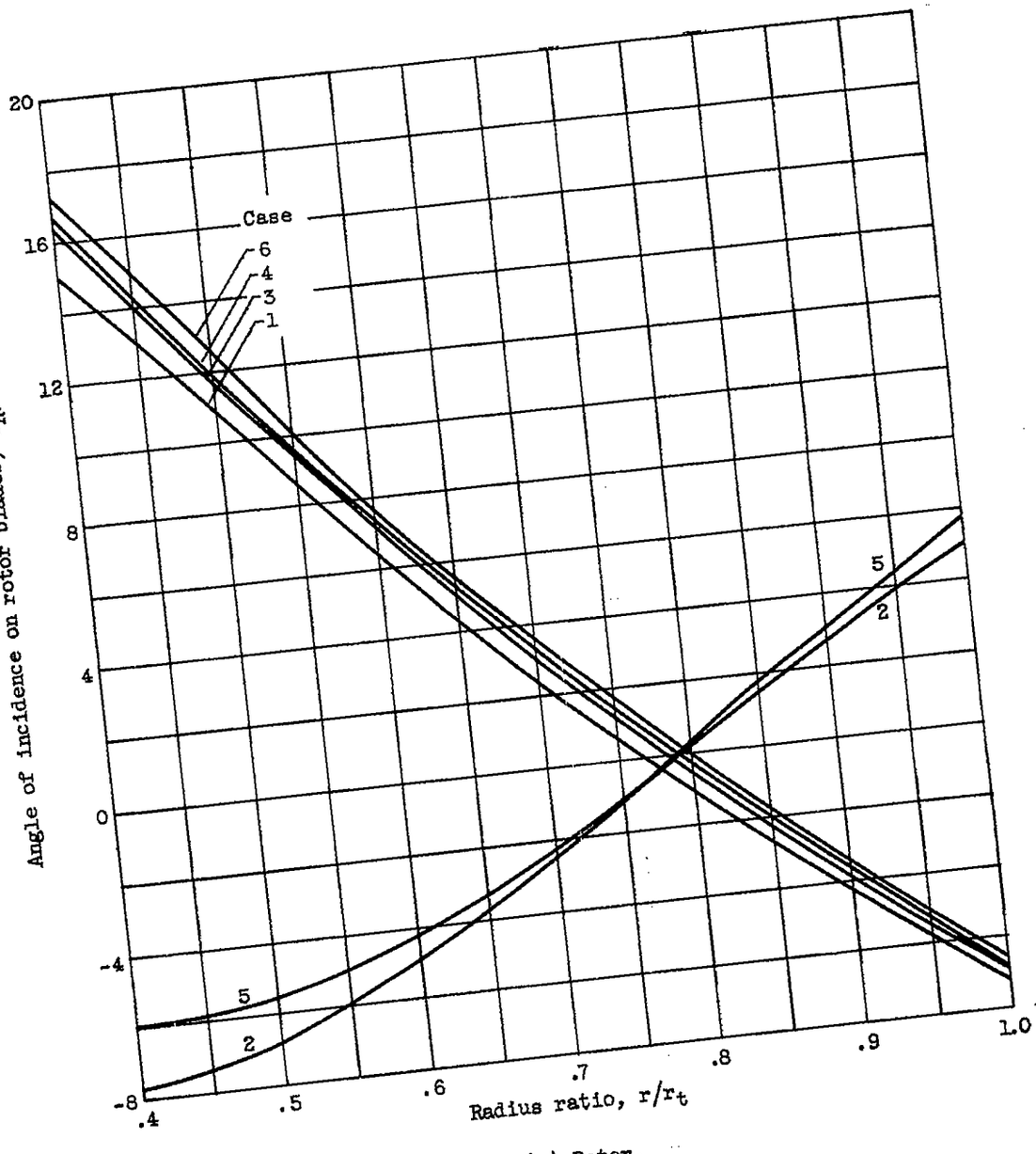

(a) Rotor.

Figure 2. - Radial variation of angle of incidence.

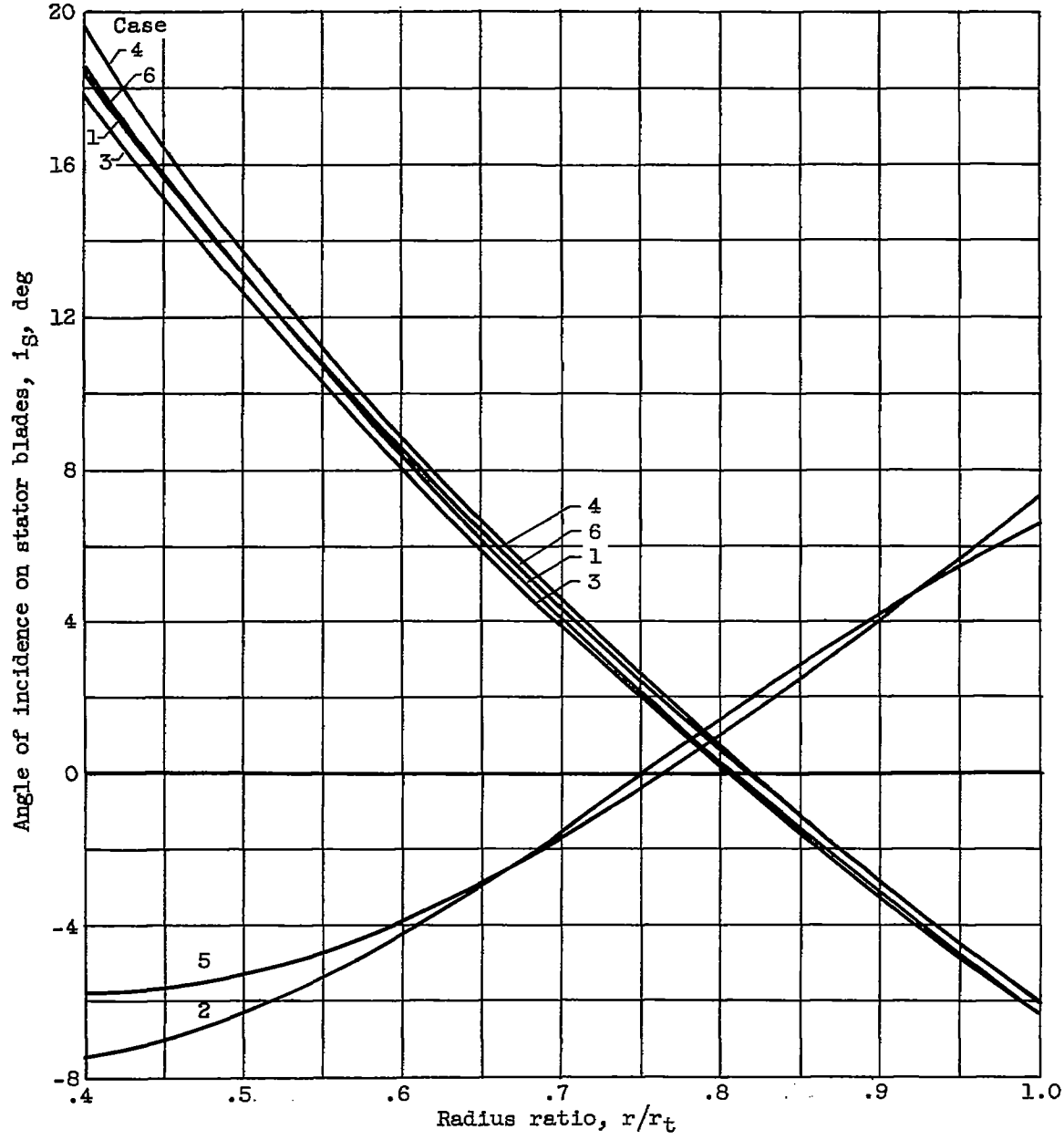

(b) Stator.

Figure 2. - Concluded. Radial variation of angle of incidence.

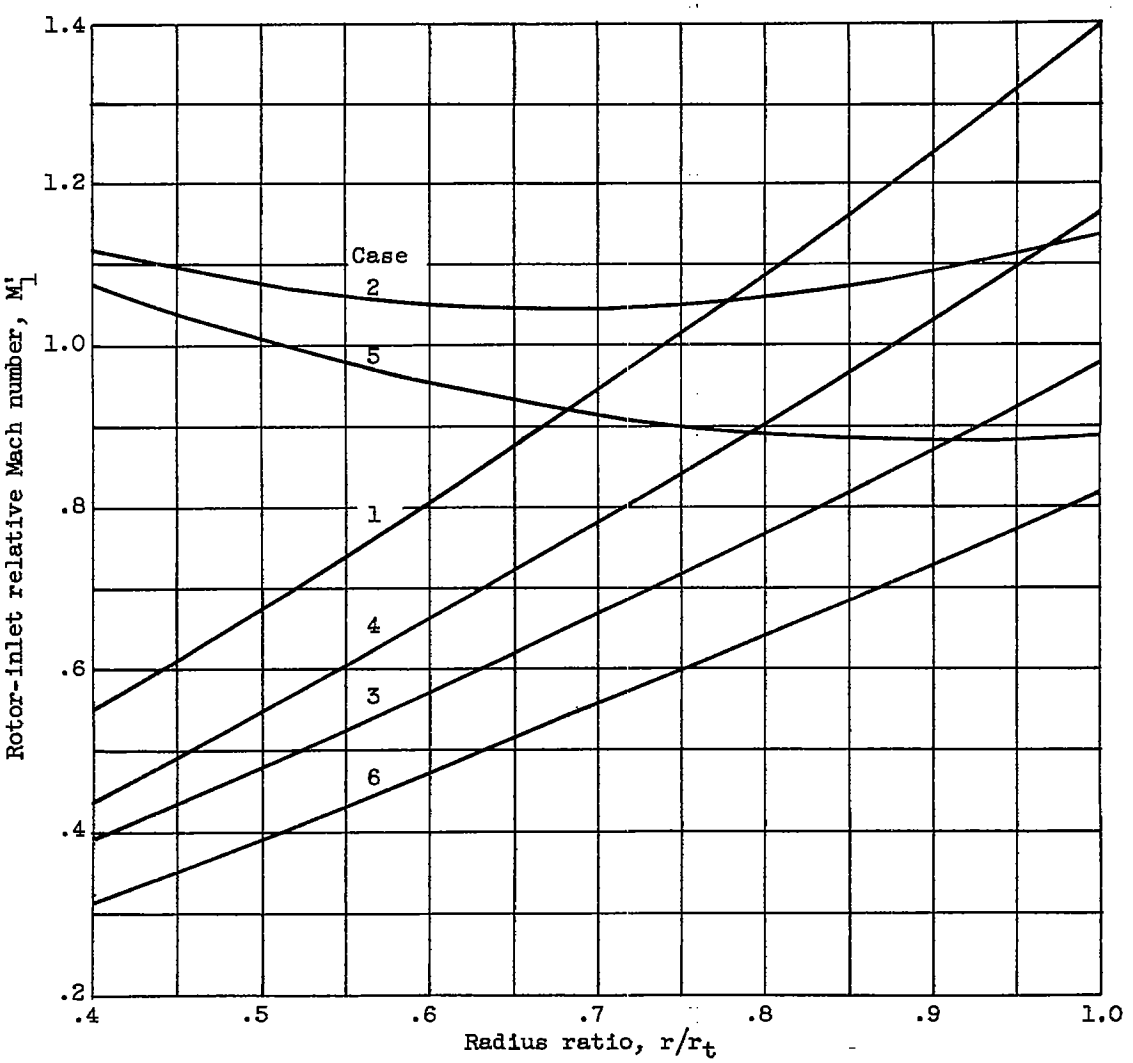

(a) Rotor.

Figure 3. - Radial variation of inlet Mach number.

4072

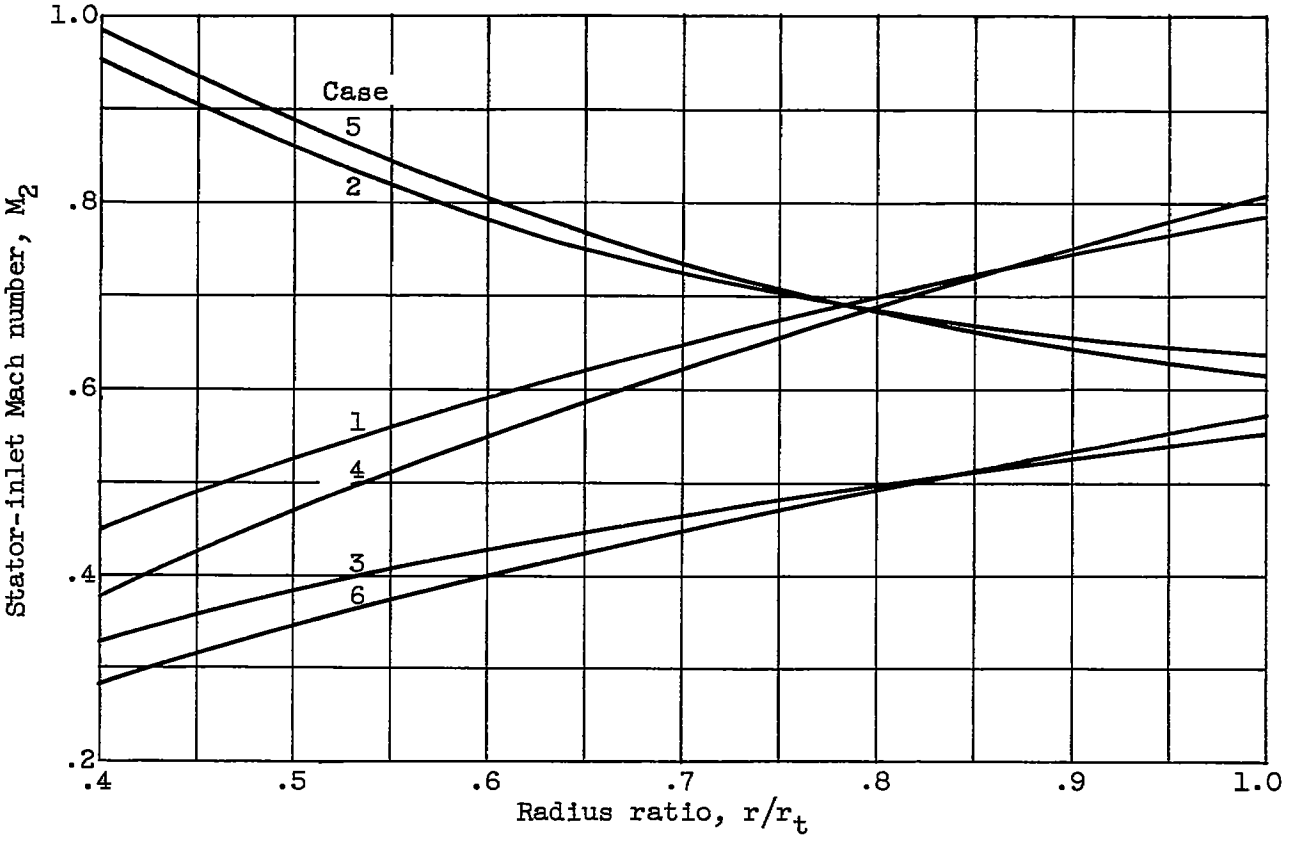

(b) Stator.

Figure 3. - Concluded. Radial variation of inlet Mach number.

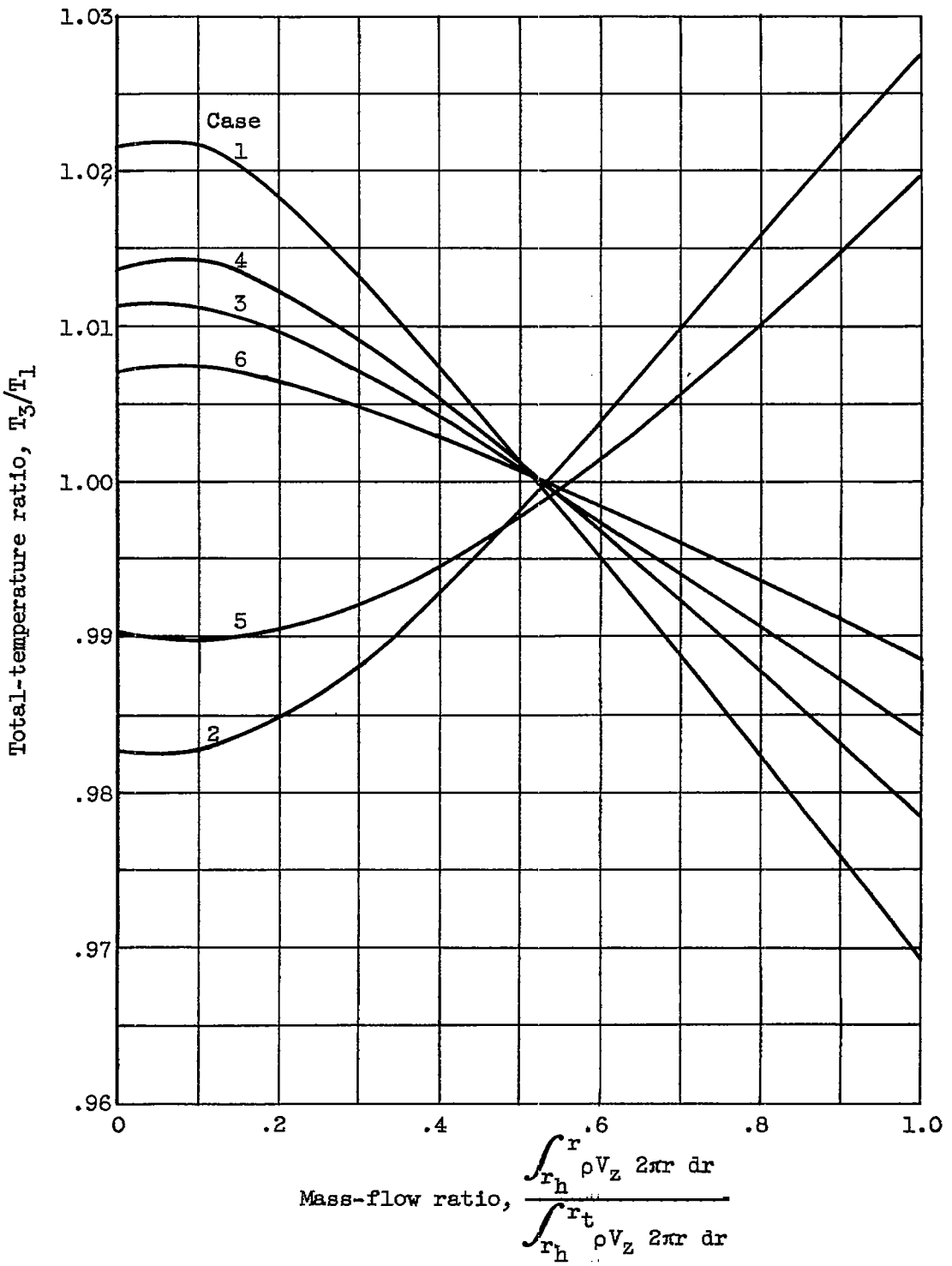

Figure 4. - Total-temperature distortion at windmill exit.

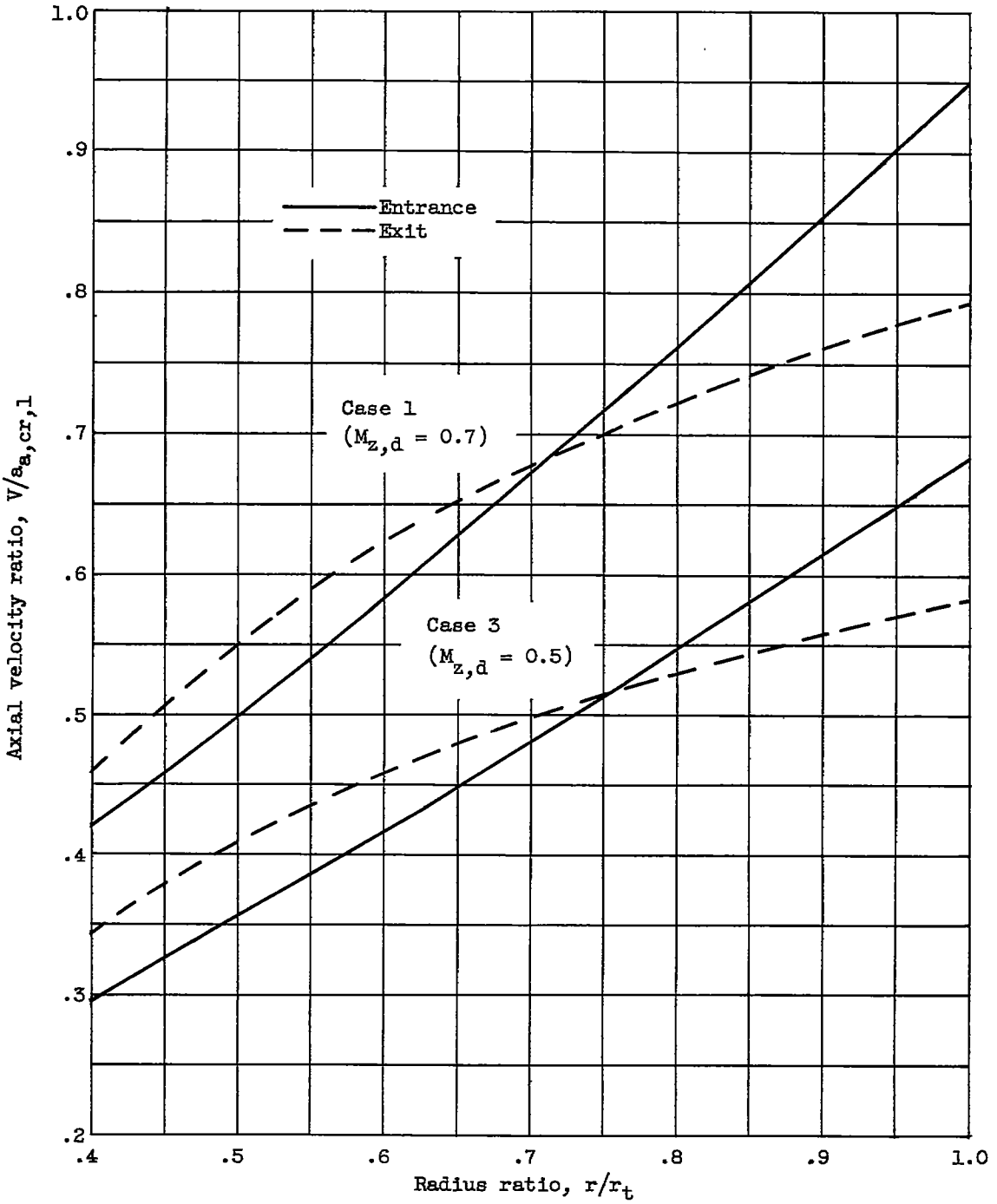

(a) Effect of axial Mach number.

Figure 5. - Radial variation of axial velocity.

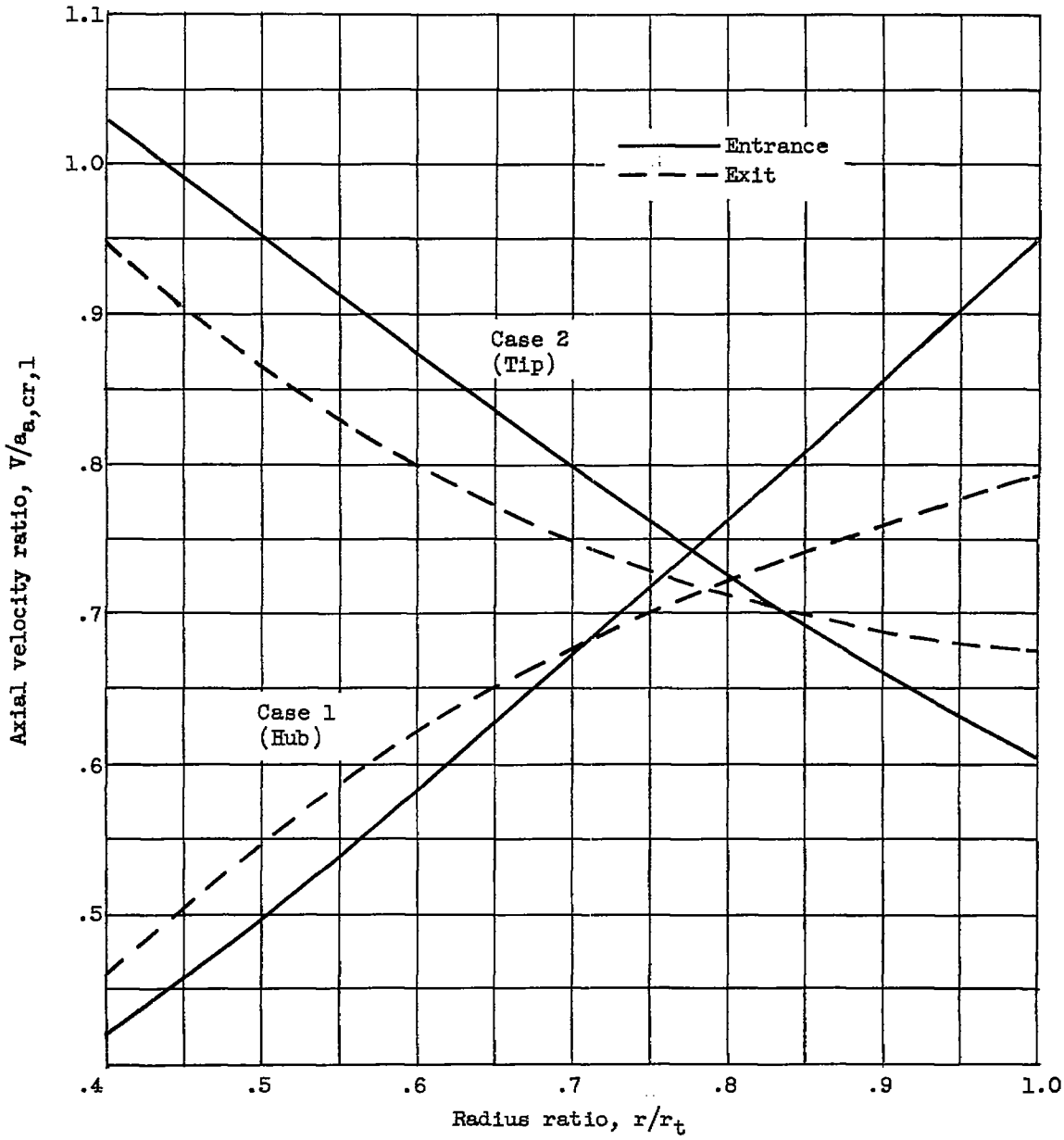

(b) Effect of location of low-velocity region.

Figure 5. - Concluded. Radial variation of axial velocity.

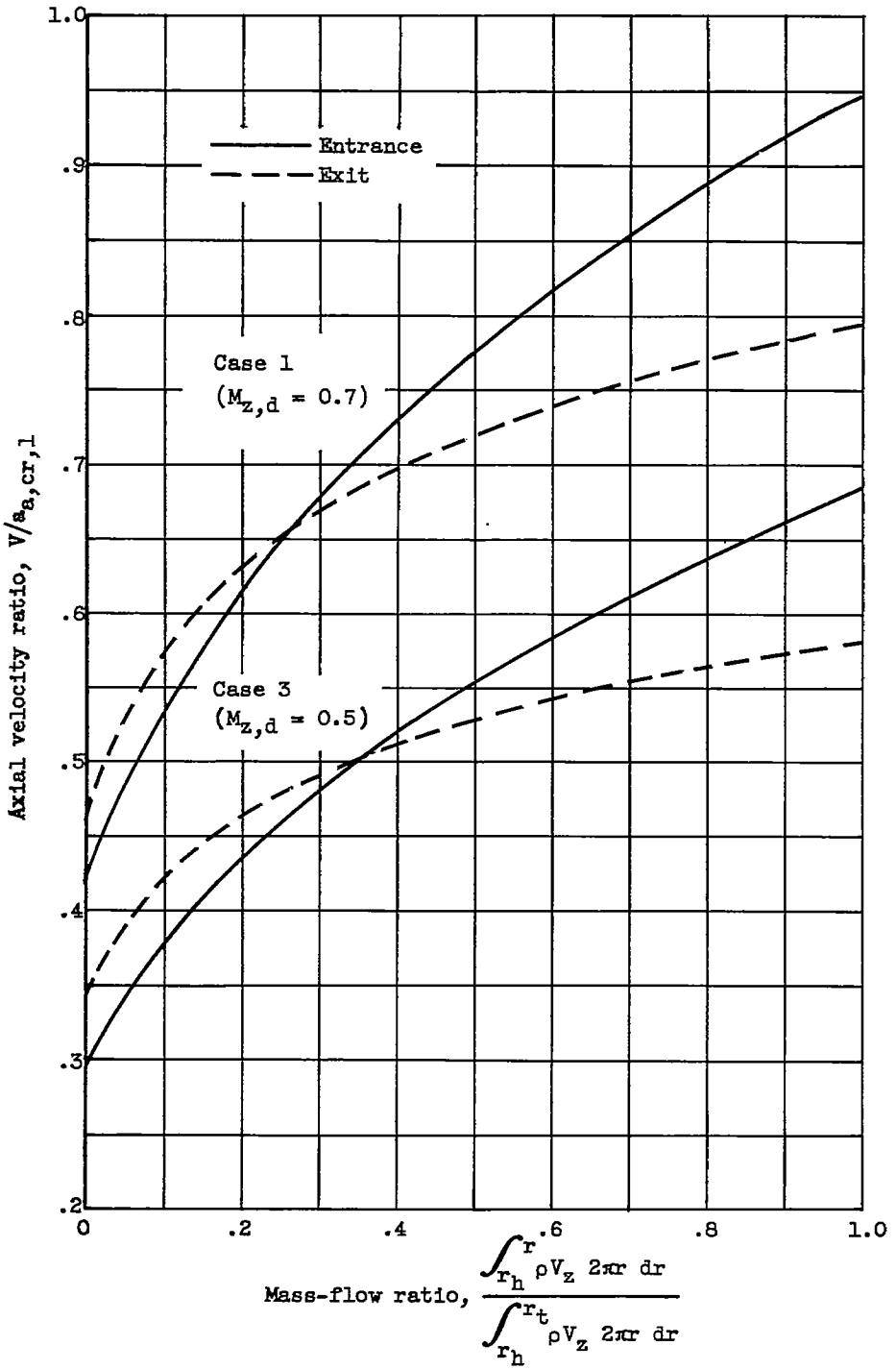

(a) Effect of axial Mach number.

Figure 6. - Variation of axial velocities with mass-flow ratio.

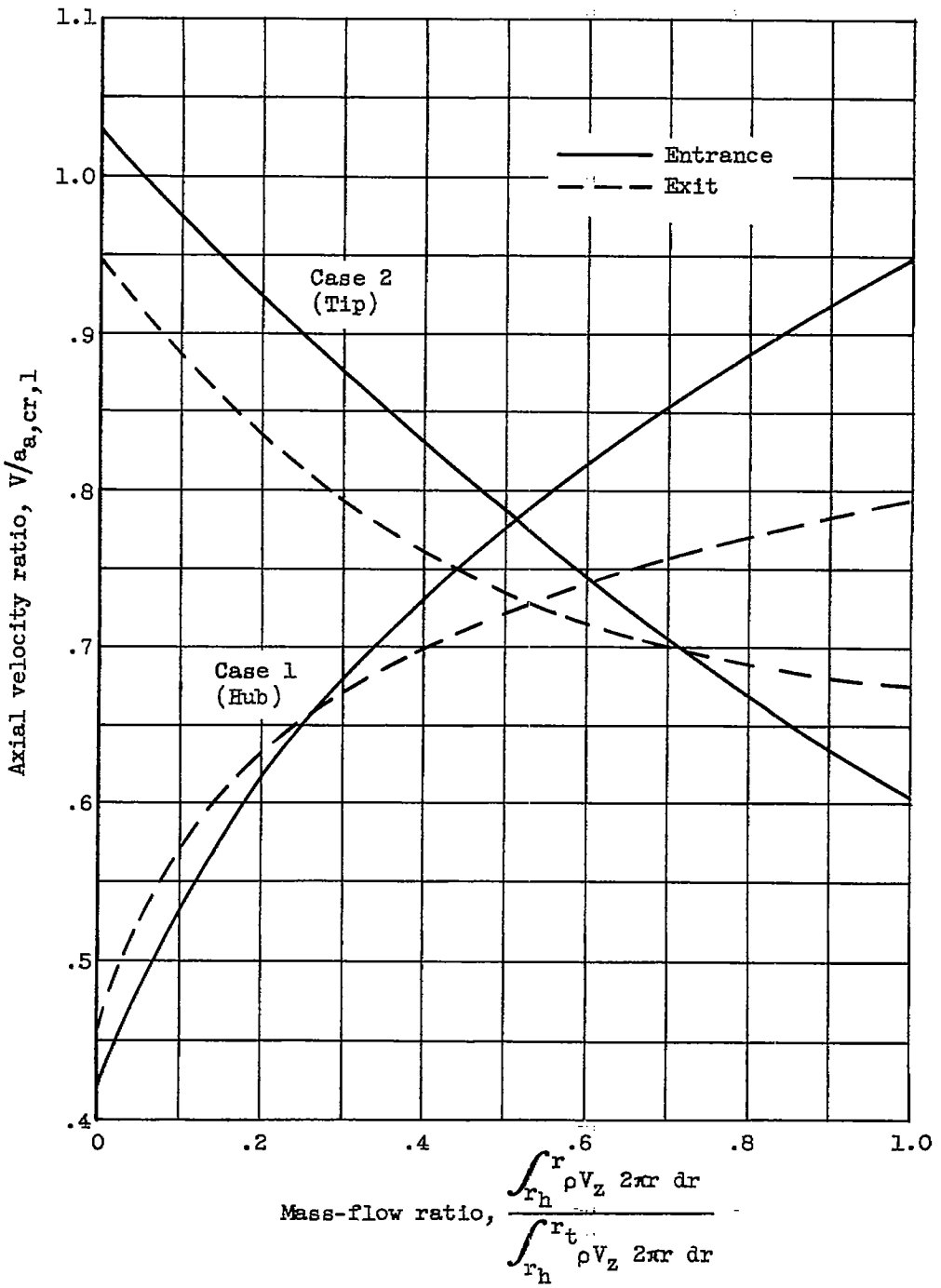

(b) Effect of location of low-velocity region.

Figure 6. - Concluded. Variation of axial velocities with mass-flow ratio.

4072

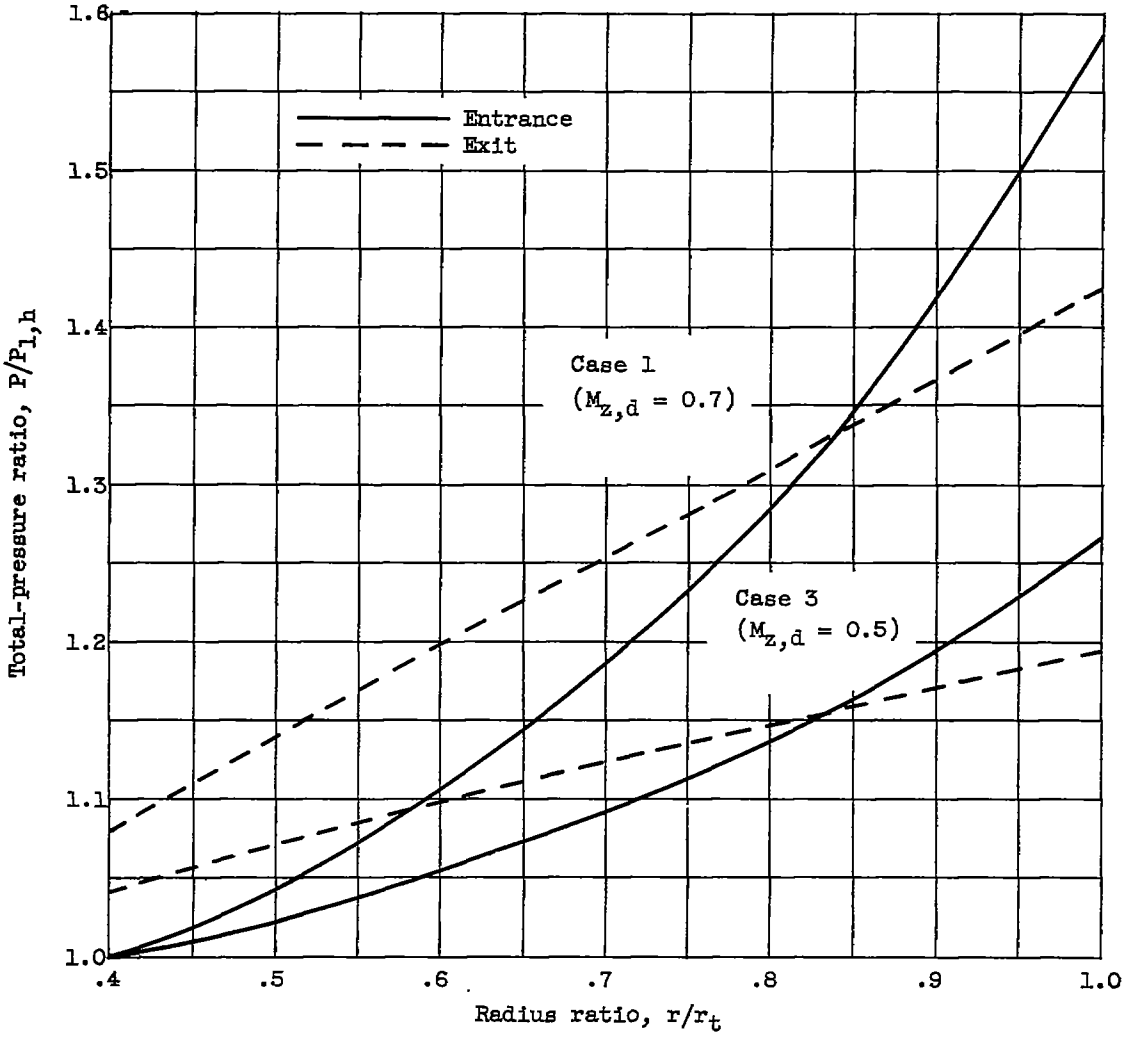

(a) Effect of axial Mach number.

Figure 7. - Radial variation of total pressure.

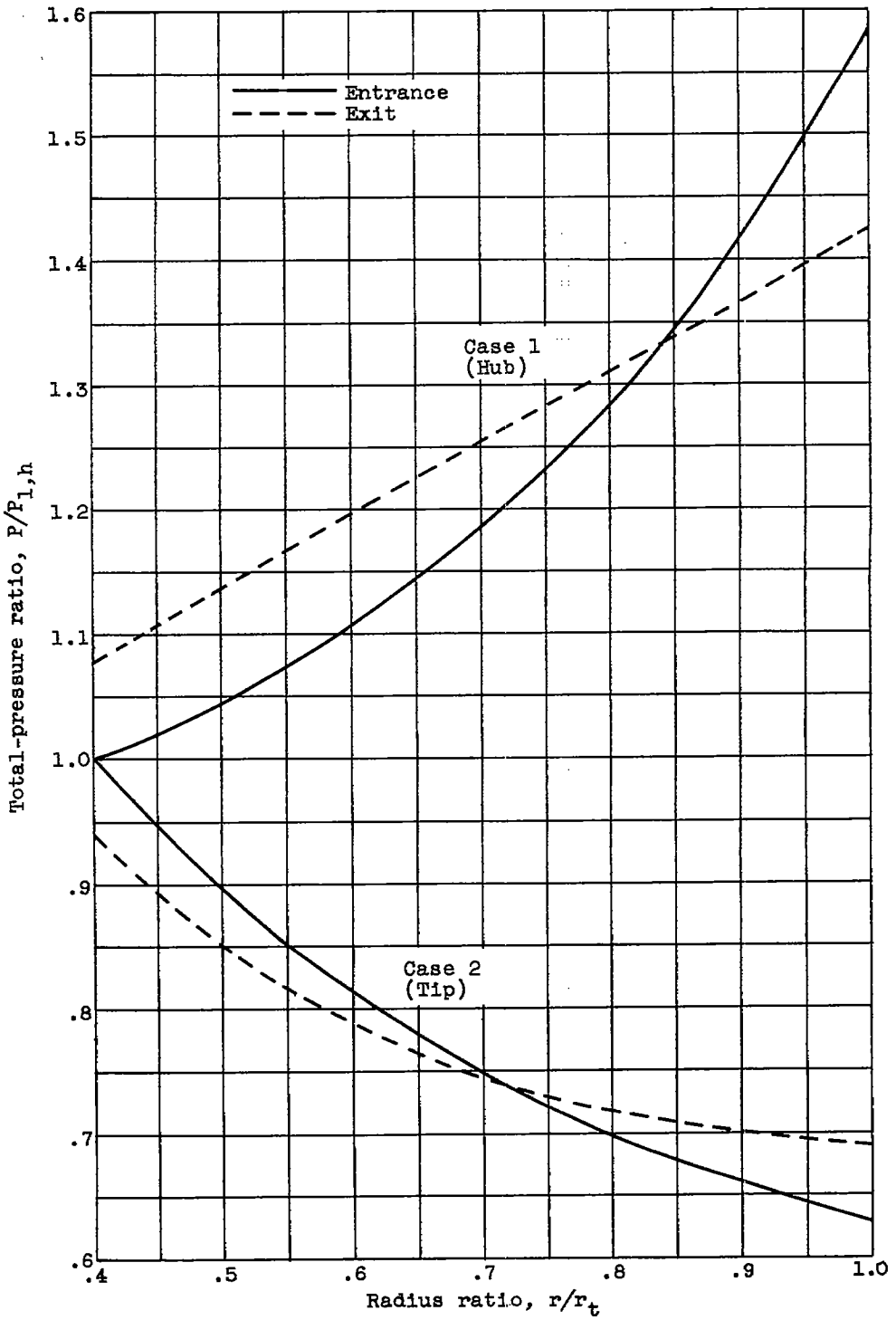

(b) Effect of location of low-velocity region.

Figure 7. - Concluded. Radial variation of total pressure.

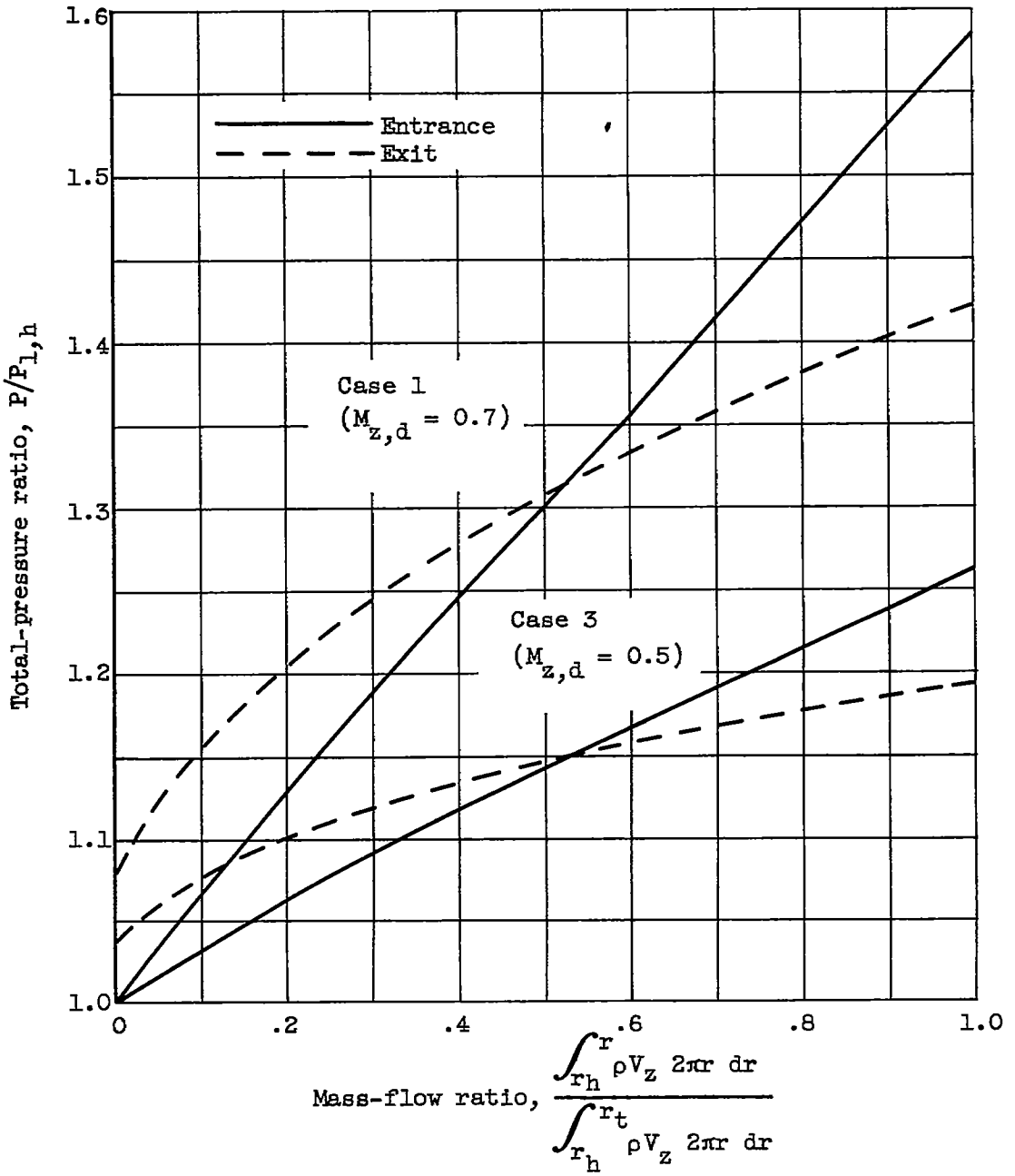

(a) Effect of axial Mach number.

Figure 8. - Variation of total pressure with mass-flow ratio.

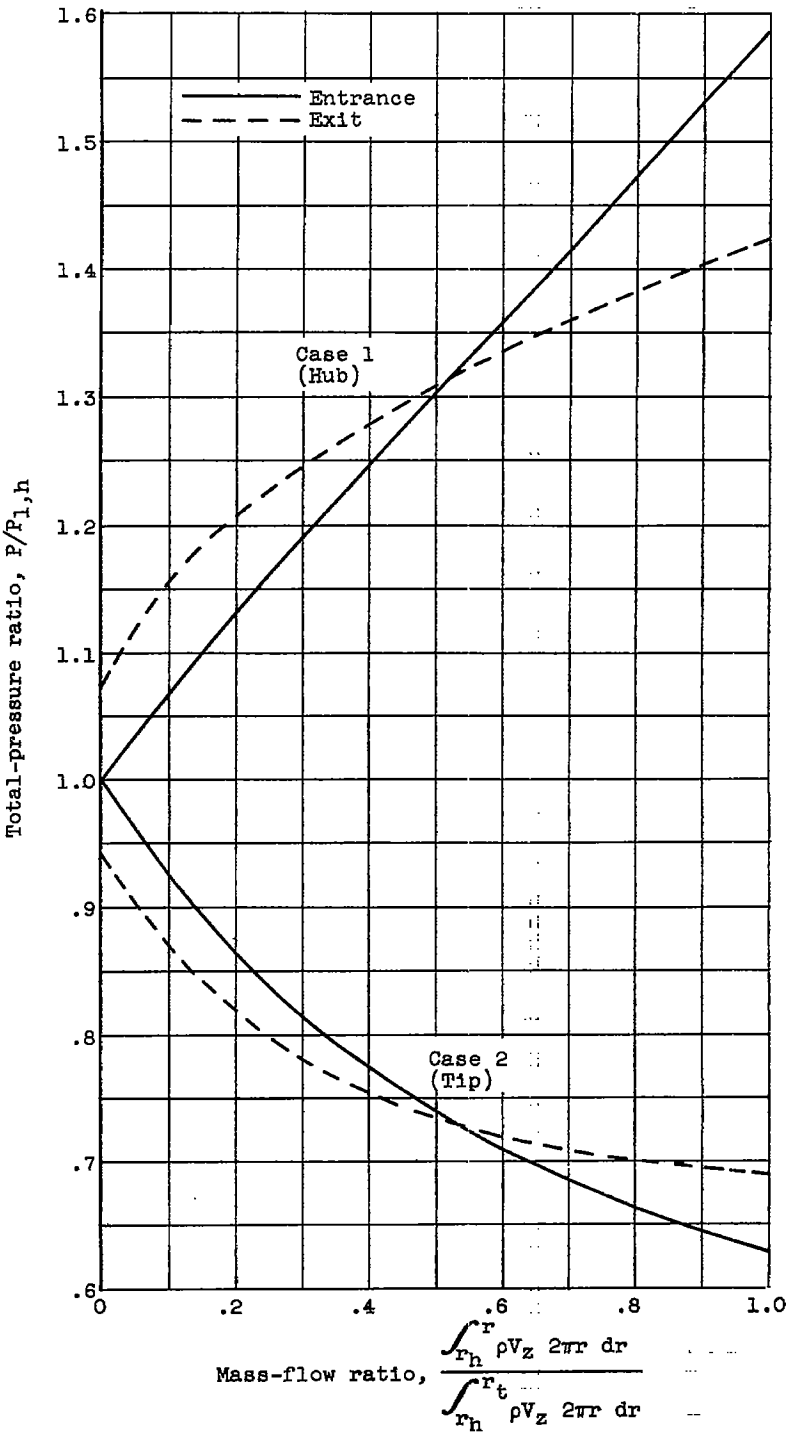

(b) Effect of location of low-velocity region.

Figure 8. - Concluded. Variation of total pressure with mass-flow ratio.